

InP based Polarization Insensitive Tunable Duplexer and Integrated Reflective Transceiver

L. Xu, X.J.M. Leijtens, M.J.H. Sander-Jochem, T. de Vries, Y.S. Oei, P.J. van Veldhoven, R. Nötzel and M.K. Smit

COBRA Research Institute, Technische Universiteit Eindhoven

Postbus 513, 5600 MB Eindhoven, The Netherlands

l.xu@tue.nl

Abstract: In this paper, a transceiver is presented which monolithically integrates a tunable wavelength duplexer, a reflective SOA (RSOA) and a detector. The first characterization shows that the tunable wavelength duplexer has less than 2 dB excess loss, better than -15 dB optical isolation between the upstream and downstream signals, and can be tuned efficiently by electro-optical ($V_{\pi} = 2.5$ V) and thermal ($I_{\pi} = 15$ mA) effects, independent of the input polarization state. A $750 \mu\text{m}$ long RSOA achieves around 20 dB on-chip gain, and a $30 \mu\text{m}$ long photodetector shows good responsivity of 0.4 A/W at -2V bias voltage.

Introduction

The single mode optic fiber has been adopted as the workhorse for the core and metropolitan networks, and is also increasingly penetrating the access domain to meet the rapidly growing bandwidth requirement for different communication services from the subscribers [1, 2]. The Dutch Broadband Photonics Access project is dedicated to providing the users with a congestion-free (first up to 1 Gbit/s, later up to 10 Gbit/s) optic fiber access network, whose capacity can be adapted according to the instantaneous and temporal user needs. In this access network, the local exchange, fig. 1, distributes two wavelengths spaced 500 GHz for each user, one for the downstream data, and the other one (CW) for later carrying the upstream data, while the spacing between the different channels in the network is 50 GHz. Thus, a transceiver (ONU) at the user site is needed not only to separate these two wavelengths, but also to detect the optical downstream data required by the user, and transmit the upstream data from the user. Since the wavelengths are decided by the local exchange, the transceiver has to be wavelength agnostic, which is why a reflective semiconductor amplifier is chosen as a transmitter. In this way, the wavelength specified by the local exchange could be amplified, modulated and reflected at the user site. Previous research [3] has demonstrated a transceiver up to 1.25 Gbit/s by using discrete components: a wave-

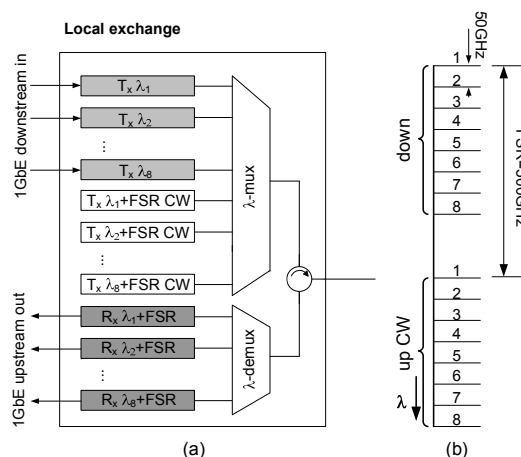


Figure 1: (a) Wavelength allocation scheme at the local exchange. (b) The spacing between the upstream and downstream channels is 500 GHz, while the spacing between the different channels in the network is 50 GHz.

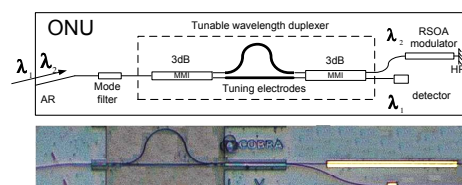


Figure 2: (Up) The layout of the integrated transceiver consisting of a wavelength duplexer, a reflective SOA consisting of a wavelength duplexer, a reflective SOA modulator and a detector. (Below) The fabricated transceiver used for characterization.

length duplexer, a RSOA as transmitter, and a photodetector. However, due to the cost, it is not practical to deploy such a transceiver at the user site.

In this paper, we present a reflective transceiver which monolithically integrates all above discrete components within one chip based on butt-joint regrowth on InP, fig. 2. The wavelength duplexer is a Mach-Zehnder (MZ) interferometer, composed of two 3 dB MMIs, connected by two waveguides with different length. The length difference between two MZ-arms is $85 \mu\text{m}$, to match the 500 GHz band spacing between each upstream and downstream channel-pair. To maximize the transmission for the upstream/downstream

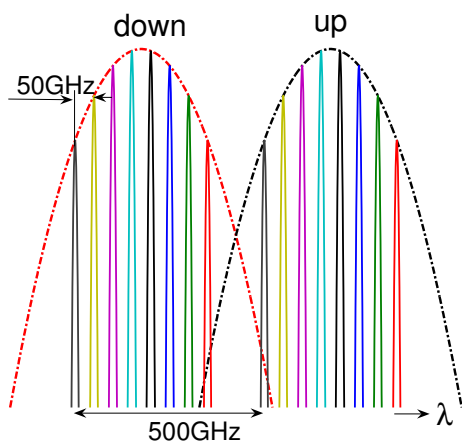


Figure 3: Incoming wavelengths from the local exchange with the passbands of the wavelength duplexer.

channel-pair selected by the local exchange, the wavelength duplexer of the transceiver has to be able to tune the proper wavelength, fig. 3. In order to tune this interferometer, both arms have been provided with 2 mm tuning electrodes. The RSOA is realized by applying a high reflectivity coating (HR) at one side of the chip. To avoid lasing, the other facet of the chip, where the light is coupled into and out of the device, is provided with an anti-reflection coating (AR). To further reduce any residual reflections, the input waveguide is placed at an angle with the chip facet, and a mode filter is inserted to filter first-order modes.

The device works as follows. Two wavelengths (λ_1 and λ_2) come from the network into the transceiver from the left side. They are spatially separated by the tunable wavelength duplexer and guided to the photodetector (λ_1) and the reflective SOA modulator (λ_2). The downstream data, carried by λ_1 , is detected by the photodetector, while λ_2 is a continuous wave (CW) light and is guided to the RSOA where it is modulated, amplified and reflected back to the network. Since the polarization state of the incoming light varies with time, the device should be polarization insensitive.

Below, we present the fabrication and measurement results of the transceiver. The tunable duplexer was tuned by both the electro-optic effect and the thermal effect for TE and TM polarization. The saturation power of the RSOA was measured at different injection currents, and the gain of the RSOA was obtained. The dependence of the photodetector responsivity on the wavelength and on the input optical power were investigated.

Fabrication and Characterization

The devices were fabricated in material grown on an N-type InP substrate by three-step low pressure metal-

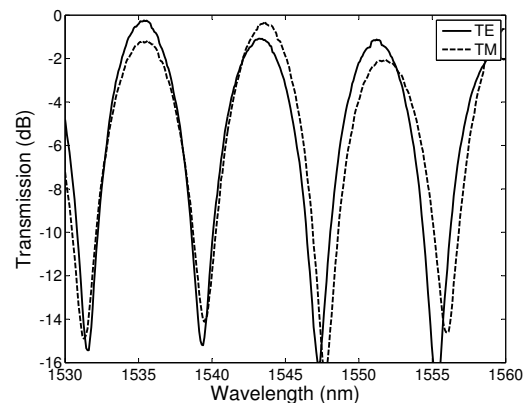


Figure 4: A polarization insensitive duplexer with 500 GHz channel spacing. Shown is the measured transmission as a function of the wavelengths.

organic-vapor-phase epitaxy (MOVPE). The first epitaxy finished with a 120 nm thick SOA active InGaAsP layer ($Q1.55$, $\lambda_{\text{gap}} = 1.55 \mu\text{m}$), embedded between two quaternary confinement layers ($Q1.25$) with different doping levels, covered by a 200 nm thick p-InP layer. Next, the active sections were defined by lithography and reactive ion etching (RIE) using a SiN_x layer as etching mask. In the second epitaxy step, a n- $Q1.25$ InGaAsP layer and a 200 nm non-intentionally-doped (n.i.d) InP buffer layer were selectively grown for the passive sections with the SiN_x mask protecting the active sections[4]. In the third epitaxy step, the p-doped InP cladding layers with graded doping level and the p-InGaAs contact layer were grown with a total thickness of 1300 nm.

All the waveguides were fabricated by RIE. Polyimide was spun for passivation and planarization. By etching back the polyimide, the p-InGaAs contact layer was exposed and Ti/Pt/Au metal layers were evaporated to form the electrodes on the top and the ground (n-InP) at the backside. After annealing and cleaving, the chip was soldered on a copper chuck with a Peltier cooler for the characterization.

For measuring the transmission of the duplexer, we used the spontaneous emission spectrum from an EDFA to couple light into the device. The spectral response was recorded with an optical spectrum analyzer. The result of the measurement is shown in fig. 4. The vertical axis shows the transmission of the duplexer, normalized to a shallowly etched straight waveguide. From the figure, we can see that the excess loss is less than 2 dB; the isolation between two datastreams is better than 15 dB; the peak transmission is insensitive to the polarization state of the light.

When a voltage is applied in reverse bias over the 2 mm long electrode on one of the MZ-arms, a change in the effective refractive index (N_{eff}) is induced by the electro-optic effects [5]. The measured values are shown in fig. 5, from which we also see a polarization insensitivity over a 5 V range. According to

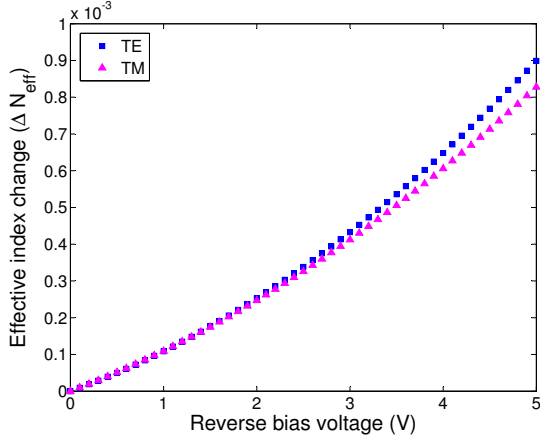


Figure 5: The extracted effective index change due to electro-optical effects as a function of the reverse bias voltage, for TE and TM polarization.

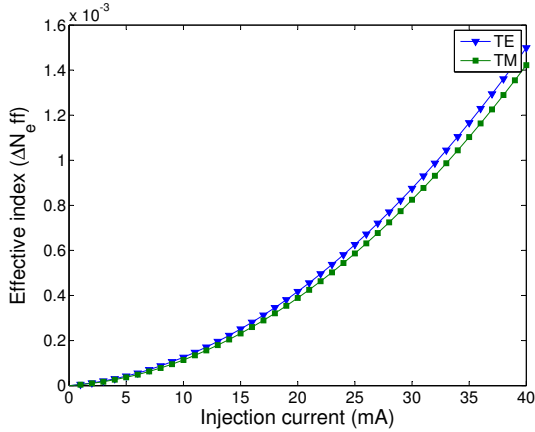


Figure 6: The extracted effective index change due to thermal effect as a function of the injection current for TE and TM polarization.

the equation $\Delta\phi = \frac{2\pi}{\lambda}\Delta N_{\text{eff}}L$, a value for $V_{\pi} \simeq 2.5$ V is obtained, for both TE and TM polarization. The polarization insensitive tuning with high efficiency under electro-optical effects are mainly due to the carrier induced effects [6], the high field confinement due to the deep etch, and a thin depletion buffer layer above the waveguide film [7].

Instead of applying a tuning voltage, we can also inject a current through the electrode, to generate heat to change the refractive index. The result, fig. 6, shows that the thermal tuning is polarization insensitive, and the tuning current for obtaining π phase shift, I_{π} , is about 15 mA for a 2 mm long gold electrode. The measurement results show that the refractive index change is linear with the injected electric power (i.e. quadratic with the injected current).

We measured the saturation power and gain of the RSOA for a device with 750 μm length. Fig. 7 shows the fiber-fiber gain for different injection currents. At the highest injection current (80 mA), the gain starts to saturate at an injection power level of -15 dBm, shifting to -10 dBm at lower injection currents. The

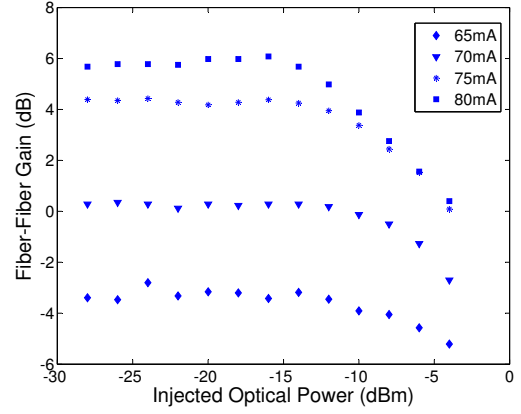


Figure 7: Fiber-fiber gain as a function of the input optical power for $\lambda = 1524$ nm at different injection currents.

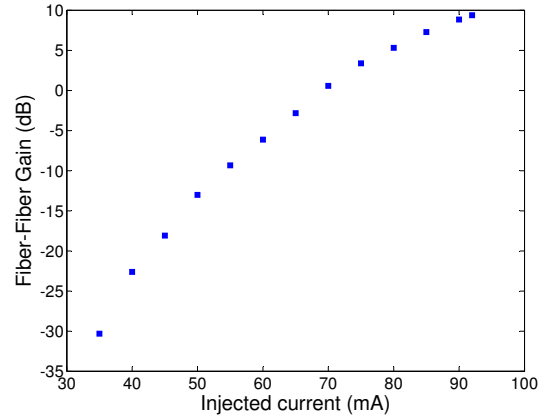


Figure 8: Small signal fiber-fiber gain (before saturation) as a function of the injection current for $\lambda = 1524$ nm. The input optical power is -18 dBm.

fiber-fiber gain for a fixed input injection power of -18 dBm is shown in fig. 8. Near the peak wavelength (1524 nm) a gain of more than 8 dB can be obtained, which is sufficient for our application. The maximum injection current is limited by the the lasing threshold of the RSOA, and the measured threshold current is about 100 mA. We believe that this can be improved by further removing residual reflections.

The modulation speed of the RSOA is limited mostly by the carrier lifetime, which is shortened with higher injection current. For an InP based SOA the carrier lifetime is on the order of hundreds of picoseconds, thus corresponding to GHz modulation rates. Koren et al. [8] have measured the modulation bandwidth of a single SOA at different injection currents, up to 3 GHz when SOA was saturated.

The photodetector has the same layer structure as the RSOA, but works under reverse bias. We fabricated detectors with lengths ranging from 30 μm to 60 μm . Here we present the measurements of the 30 μm -long and 2 μm -wide detector. The dark current of the photodetector is less than 50 nA at -5 V reverse bias voltage. The measured responsivity, shown in fig. 9, is ~ 0.4 A/W at -2 V bias. This corresponds to $\sim 90\%$ in-

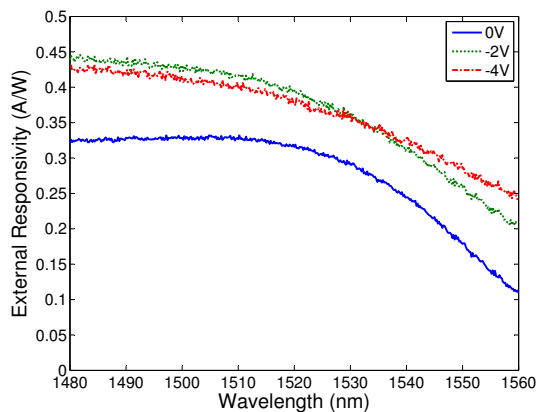


Figure 9: Responsivity of $30\mu\text{m}$ long detector as a function of the wavelength at difference reverse bias voltages.

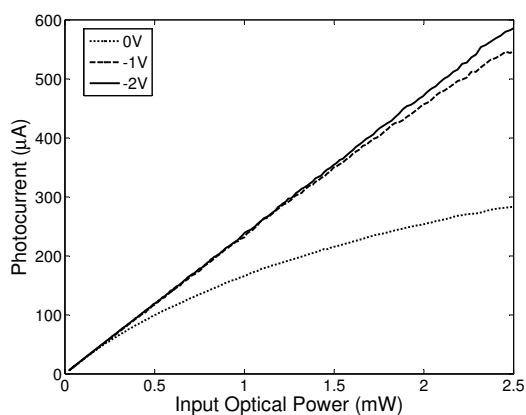


Figure 10: The photocurrent as a function of the input optical power input from the angled input side for a $30\mu\text{m}$ long photodetector at $\lambda_{\text{peak}} = 1515.18\text{ nm}$.

ternal quantum efficiency if the fiber chip coupling loss is estimated at -4.3 dB . The photocurrent increases linearly with the input optical power up to more than 4 dBm (2.5 mW) when the photodetector is reversely biased, shown in fig. 10. The estimated bandwidth for this detector is up to 25 GHz based on RC time and carrier-transit time calculation.

Conclusion

In this paper, we reported a monolithically integrated transceiver that consists of a polarization insensitive tunable duplexer, a RSOA modulator and a photodetector. The tunable duplexer has less than 2 dB excess loss and gives better than 15 dB isolation between the downstream and upstream data channels. Polarization insensitive tuning is realized by employing both the electro-optic effects ($V_{\pi} \approx 2.5\text{ V}$) and the thermal effect ($I_{\pi} = 15\text{ mA}$). The transceiver obtained more than 8 dB fiber-fiber gain at 90 mA injection current, and a good responsivity of $\sim 0.4\text{ A/W}$ for a $30\mu\text{m}$ -long photodetector, at -2 V reverse bias.

Acknowledgment

This work is funded by the Dutch National Broadband Photonics Access project and by the Netherlands Organization for Scientific Research (NWO) through the “NRC Photonics” grant.

References

- [1] T. Koonen, “Fiber to the home/fiber to the premises: What, where, and when?” *Proceedings of the IEEE*, vol. 94, no. 5, pp. 911–934, 2006.
- [2] H. Shinohara, “Broadband access in Japan: rapidly growing FTTH market,” *IEEE Comm. Magazine*, vol. 43, no. 9, pp. 72–78, Sept. 2005.
- [3] J. Prat, C. Arellano, V. Polo, and C. Bock, “Optical network unit based on a bidirectional reflective semiconductor optical amplifier for fiber-to-the-home networks,” *IEEE Photon. Technol. Lett.*, vol. 17, no. 1, pp. 250–252, Jan. 2005.
- [4] Y. Barbarin, E. Bente, C. Marquet, E. Lecère, T. de Vries, P. van Veldhoven, Y. Oei, R. Nötzel, M. Smit, and J. Binsma, “Butt-joint reflectivity and loss in InGaAsP/InP waveguides,” in *Proc. 12th Eur. Conf. on Int. Opt. (ECIO '05)*. Grenoble, France, April 6–8 2005, pp. 406–409.
- [5] H. Zappe, *Introduction to Semiconductor Integrated Optics*. Boston: Artech House Publishers, 1995, ISBN 0-089006-789-9.
- [6] J. Vinchant, J. Cavaillès, M. Erman, P. Jarry, and M. Renaud, “InP/InGaAsP guided-wave phase modulators based on carrier-induced effects: theory and experiment,” *J. Lightwave Technol.*, vol. 10, no. 1, pp. 63–69, 1992.
- [7] D. Maat, “InP-based integrated MZI switches for optical communications,” Ph.D. dissertation, Delft University of Technology, Delft, The Netherlands, 2001, ISBN 90-9014700-4.
- [8] U. Koren, B. Miller, M. Young, T. Koch, R. Jopson, A. Gnauck, J. Evankow, and M. Chien, “High frequency modulation of strained layer multiple quantum well optical amplifiers,” *Electron. Lett.*, vol. 27, no. 1, pp. 62–64, Jan. 1991.